Published in final edited form as:

Acta Biomater. 2018 May ; 72: 228–238. doi:10.1016/j.actbio.2018.03.056.

Anisotropic Biodegradable Lipid Coated Particles for Spatially Dynamic Protein Presentation

Randall A. Meyer[A,B,C,†], **Mohit P. Mathew**[A,B,†], **Elana Ben-Akiva**[A,B], **Joel C. Sunshine**[A,B], **Ron B Shmueli**[A,B], **Qiuyin Ren**[A,B], **Kevin J. Yarema**[A,B], and **Jordan J. Green**[A,B,C,D,E,F,G,H,*]

[A]Department of Biomedical Engineering, Johns Hopkins University School of Medicine, Baltimore, MD, 21231, USA

[B]Translational Tissue Engineering Center, Johns Hopkins University School of Medicine, Baltimore, MD, 21231, USA

[C]Institute for Nanobiotechnology, Johns Hopkins University School of Medicine, Baltimore, MD, 21231, USA

[D]Department of Materials Science and Engineering, Johns Hopkins University School of Medicine, Baltimore, MD, 21231, USA

[E]Department of Ophthalmology, Johns Hopkins University School of Medicine, Baltimore, MD, 21231, USA

[F]Department of Oncology, Johns Hopkins University School of Medicine, Baltimore, MD, 21231, USA

[G]Department of Neuroscience, Johns Hopkins University School of Medicine, Baltimore, MD, 21231, USA

[H]Department of Chemical and Biomolecular Engineering, Johns Hopkins University School of Medicine, Baltimore, MD, 21231, USA

Abstract

There has been growing interest in the use of particles coated with lipids for applications ranging from drug delivery, gene delivery, and diagnostic imaging to immunoengineering. To date, almost all particles with lipid coatings have been spherical despite emerging evidence that non-spherical shapes can provide important advantages including reduced non-specific elimination and increased target-specific binding. We combine control of core particle geometry with control of particle surface functionality by developing anisotropic, biodegradable ellipsoidal particles with lipid coatings. We demonstrate that these lipid coated ellipsoidal particles maintain advantageous

[*]Corresponding author: Dr. Jordan J. Green, 400 N Broadway, Smith 5017, Baltimore, MD 21231, T: 1-410-614-9113, F: 1-443-287-6298, green@jhu.edu.

[†]These authors contributed equally to this work.

Disclosures: The authors do not have any competing interests to disclose.

properties of lipid polymer hybrid particles, such as the ability for modular protein conjugation to the particle surface using versatile bioorthogonal ligation reactions. In addition, they exhibit biomimetic membrane fluidity and demonstrate lateral diffusive properties characteristic of natural membrane proteins. These ellipsoidal particles simultaneously provide benefits of non-spherical particles in terms of stability and resistance to non-specific phagocytosis by macrophages as well as enhanced targeted binding. These biomaterials provide a novel and flexible platform for numerous biomedical applications.

Graphical abstract

Keywords

lipids; polymers; membrane fluidity; particle shape; biomimetic

1. Introduction

Lipid polymer hybrid particles, that combine the biomimetic cellular surface features of a liposome with the structural support and stability of a polymeric particle, have been of great interest to the biomaterials community in recent years. Generally, these constructs are of core-shell design with the polymer encapsulating various therapeutics in the core, and naturally or synthetically derived lipids forming a shell. By fusing a preformed lipid vesicle to a polymeric particle [1] or taking advantage of self-assembling lipid bilayers during particle synthesis [2], these particles can be fabricated with a variety of different strategies depending on the desired application.

The lipid polymer hybrid particle technology holds tremendous promise and has already been demonstrated in several applications [3] including drug delivery [4], diagnostic imaging [5], and gene delivery [6, 7]. Furthermore, this lipid coating strategy has been extended to the synthesis of polymeric nanoparticles containing membranes derived from red blood cells [8], platelets [9], and cancer cells [10]. Polymeric particles with naturally derived membranes have been shown to be useful for many other applications including adsorption of hemolytic toxins [11], pathogen binding [9], and cancer cell antigen delivery for vaccines [10].

One particle design limitation of this approach, however, has been that, up to now, almost all lipid coated particles have been of isotropic, spherical shape. Yet, emerging evidence suggests that that non-spherical micro- and nanoparticles possess several key advantages over traditional spherical particles which include inhibited non-specific cellular uptake [12] and simultaneously potential enhanced target-specific binding and cell uptake [13]. As a result, anisotropic particles have been appropriated for several recent biological applications

such as anti-cancer drug delivery [14, 15], gene delivery *in vitro* and *in vivo* [6, 16, 17], and immunoengineering to stimulate T-Cells against tumor associated antigens [18, 19]. In all of these applications, the non-spherical anisotropic particle has been shown to be superior to the isotropic spherical particle.

To investigate the feasibility of combining these previously separate particle technologies—the use of anisotropic shapes in particle core design and the hybridization of lipids on polymeric particles for dynamic surfaces—we developed a procedure to reproducibly generate non-spherical, ellipsoidal lipid coated particles with a biodegradable polymer support. The process includes generating non-spherical particles, which can be manufactured from both top-down [13] and bottom-up methods [20]. In the current work, we utilized, as outlined in Scheme 1, a thin film stretching method developed by Ho et. al. [21] that we recently automated [22] with an electromechanical stretching device to robustly generate ellipsoidal anisotropic microparticles to serve as the support for the lipids. Next, the ellipsoidal lipid coated particles were generated by fusing 200 nm liposomes to these particles under sonication. Subsequently, the lipid surfaces were functionalized in a flexible manner through the use of biotinylated biomolecules. These new biomaterials, anisotropic biodegradable particles that exhibit resistance to non-specific cellular internalization and enable spatially dynamic protein presentation from their surfaces, are promising as biotechnology devices for delivery and diagnostic applications.

2. Materials and methods

2. 1. Particle preparation and characterization

Acid terminated poly(lactic-co-glycolic acid) (PLGA- 85:15 L:G ratio, MW 45,000 Da – 55,000 Da) (Akina Inc.; West Lafayette, IN) was dissolved in 5 mL of dichloromethane (DCM) at a concentration of 20 mg/mL. In order to visualize particles under fluorescence microscopy, 7-amino-4-methyl coumarin (7-AMC- Sigma-Aldrich; St. Louis, MO) or Nile Red (Life Technologies; Grand Island, NY) were added to the DCM solution at a 1% w/w ratio to the polymer. The resulting solution was homogenized by a T-25 digital ULTRA-TURRAX IKA tissue homogenizer at 5,000 rpm for 1 min in 50 mL of 1% poly(vinyl alcohol) (PVA) solution (IKA Works; Wilmington, NC). The subsequent emulsion was then transferred to 100 mL of 0.5% PVA solution agitated by magnetic stirbar and the DCM was allowed to evaporate over the course of 4 h. The suspended particles were centrifuged out of solution at 3000g for 5 min and washed 3 times with water. The resulting particles were flash frozen in liquid nitrogen and lyophilized prior to use.

To synthesize non-spherical ellipsoidal particles, we utilized the thin film stretching method developed by Ho et. al [21]. Spherical particles synthesized by emulsion were suspended into a solution of 10% PVA and 2% glycerol at a concentration of 5 mg/mL and 10 mL of this solution was deposited into a rectangular petri dish. The film was allowed to dry overnight, and the next day the film was cut to size and mounted onto an automated thin film stretching device [22]. The entire apparatus was heated up to 90 °C and the film was stretched 2-fold in one direction to produce ellipsoidal particles with a major axis roughly 2 times the original particle diameter and a minor axis roughly 0.7 times the original particle diameter. After stretching, the film was allowed to cool back down to room temperature and

then was dissolved in water. Particles were washed and subsequently lyophilized prior to use and characterization.

Particle characterization was conducted using scanning electron microscopy (Leo FESEM). Lyophilized particles were mounted onto an aluminum tack (Electron Microscopy Services; Hatfield, PA) using carbon tape (Nisshin EM Co.; Tokyo, Japan). The particles were then sputter coated with 30 nm of gold-palladium alloy. After sputter coating, the particles were imaged by SEM. Particle size and aspect ratio data were obtained by ImageJ analysis of the subsequent SEM images.

2.2 Lipid coated particle preparation and imaging

Non-spherical lipid coated particles were prepared utilizing a two-step method similar in concept to what has previously described for spherical particles [23]. 1,2-dioleoyl-sn-glycero-3-phosphocholine (DOPC) and cholesterol (Avanti Polar Lipids; Alabaster, AL) were mixed into a 70:30 w/w ratio. For fluorescent lipid imaging studies, rhodamine conjugated DOPC (Avanti Polar Lipids; Alabaster, AL) was mixed with DOPC, and cholesterol in a 1:69:30 w/w ratio. For surface functionalization, 1,2-dioleoyl-sn-glycero-3-phos phoethanolamine-N-[4-(p-maleimidomethyl) cyclohexane-carboxamide] (MCC-DOPC) (Avanti Polar Lipids; Alabaster, AL), DOPC, and cholesterol were mixed in a 35:35:30 w/w ratio. A total of 1 mg of the lipids was aliquoted and left to dry into a thin film overnight under a vacuum. The lipids were then hydrated in 1 mL of water The lipids were heated to 60 °C and extruded through a 200 nm filter (Avanti Polar Lipids; Alabaster, AL). Liposome formation was verified with sizing at 200 nm using dynamic light scattering (Malvern Instruments; Westborough, MA). The liposomes were then mixed with spherical or non-spherical particles (in a 33.4 μg liposome to 1 mg particle ratio) and sonicated for 30 s at 2 W power in a 1.5 mL Eppendorf tube. Temperature was maintained at 4 °C with an aluminum cooling block (Light Labs; Dallas, TX). The subsequent lipid coated particles were purified from solution through centrifugation at 4 °C for 5 min at 300g. After three washes, the lipid coated particles were stored at 4 °C until further use.

To analyze the formation of lipid constructs on the particle surface, confocal imaging of PLGA particles encapsulating 7-AMC were coated with rhodamine lipid containing liposomes. Confocal image acquisition was completed with a Zeiss 780 FCS Confocal Microscope. To derive profile information, we used the ImageJ profile measurement tool and drew a line through the particle to determine relative fluorescence information.

2.3 Cellular uptake studies

RAW 264.7 (ATCC) macrophages were cultured in T-175 flasks in Dulbecco's Minimal Essential Media (Life Technologies; Grand Island, NY) supplemented with 10% fetal bovine serum and penicillin/streptomycin. For flow cytometry studies, cells were harvested through the gentle use of a cell scraper (to prevent excessive cell damage) and seeded into 96-well plates at a density of 30,000 cells/well. After cell adherence, the cells were stained with Vybrant CFDA-SE Cell Tracer Kit following the manufacturer's protocol (Life Technologies; Grand Island, NY) as a counterstain to identify live cells in flow cytometry. The cell media was removed and replaced with 500 μL of cell media containing either

spherical or ellipsoidal particles encapsulating 5(6)-carboxy-tetramethyl-rhodamine (Merck KGaA; Darmstadt, GE) in a 2-fold dilution series starting at 0.5 mg particles/mL. The cells were then incubated for 4 hr at 37 °C for uptake studies and 4 °C for binding studies and washed 3× with PBS to remove free particles. The cells were dissociated from the plate by vigorous trituration prior to analysis by flow cytometry. Cell viability was evaluated after 24 and 48 hr in separate but identical experimental setups incubation using a cell titer kit (Promega; Madison, WI) following the manufacturer's protocol. The cells were incubated with the cell titer reagent for 1 hr and assessment of viability was conducted via relative absorbance measurements.

For confocal imaging, cells were seeded at the same concentration and incubated with 0.125 mg particles/mL of fluorescently labeled particles (corresponding roughly to 10 particles/cell), except the incubation was conducted in LabTek Chamber slides (Fisher Scientific; Pittsburgh, PA). The cells were washed 3× with PBS and then fixed in 10% formalin stabilized with methanol for 15 min (Sigma-Aldrich; St. Louis, MO). After fixing, actin was stained with Alexa 488 Phalloidin (Life Technologies; Grand Island, NY) and the nucleus was visualized with DAPI stain (BioChemica; Darmstadt, Germany), both following the manufacturer's protocol. The cells were then visualized using confocal microscopy on a Zeiss 780 FCS.

2.4 Surface protein conjugation and characterization

In order to functionalize the lipid coated particles to be receptive to protein conjugation, we first functionalized the surface with thiolated avidin (Protein Mods; Madison, WI). We first were interested in whether or not the avidin could conjugate to the surface of the maleimide activated particle. We pre-conjugated biotinylated fluorescein (Sigma- Aldrich; St. Louis, MO) with the avidin and then dialyzed overnight with a 10 kDa MWCO dialysis bag (Life Technologies; Grand Island, NY). The particles were then reacted overnight with various amounts of fluorescent avidin and washed three times. Fluorescence intensity was measured under a plate reader and correlated to the amount of fluorescent avidin on the surface of the particle.

To evaluate our capabilities to conjugate a target biotinylated protein to the surface of our lipid coated particles, we formed the lipid coated particles of ellipsoidal and spherical shape and conjugated them to the thiolated avidin overnight at 4 °C at a 4 μg avidin/mg PLGA ratio. We then conjugated Cy5-biotin (Click Chemistry Tools; Scottsdale, AZ) at a concentration of 4 μg Cy5-biotin/mg PLGA ratio for 1 h at room temperature. After washing 3 times at 4 °C, we evaluated the conjugation through confocal imaging of the particles.

To confirm that this method would work for a bioactive protein, we utilized biotinylated anti-CD28 as a model protein for particle surface capture. Avidin functionalized lipid coated particles were prepared as previously, but instead of a fluorophore, we added the protein at various concentrations to test reaction efficiency. To quantitate the amount of protein bound to the surface, we washed the particles 3 times, collected the supernatants, and analyzed them for a reduction in protein content utilizing an Octet Red system (Forte Bio; Menlo Park, CA). Reduction in protein content in the supernatant was then converted to protein

immobilized on the surface through subtraction from the total amount of protein added into the system.

2.5 Targeted anisotropic lipid coated particle binding

In order to evaluate the capability of anisotropic lipid coated particles to mediate enhanced targeted cell binding compared to spherical lipid coated particles, we prepared TAMRA loaded sperical and prolate ellipsoidal microparticles coated with MCC-lipids were synthesized as described in Section 2.1 and 2.2. Particles were then conjugated to anti-CD3 (OKT3 clone) as described in Section 2.4. Jurkat T-Cells were labeled with Vybrant CFDA SE Cell Tracer Kit (CFSE) (Life Technologies; Grand Island, NY) following the manufacturer's protocol. The particles were then incubated at a concentration of 0.1 mg/mL with 100,000 Jurkat T-Cells in 100 uL of T-Cell culture media formulated as described previously [18] for 1 hr. To evaluate binding the samples were then imaged by confocal microscropy on a Zeiss 800 FCS Confocal Microscope. A total of 10 images were taken per sample and analyzed for binding frequency and area of contact between particles and cells using Image J.

2.6 FRAP Analysis

In order to confirm the fluidic character of the spherical and ellipsoidal lipid coated particles, diffusivity was evaluated utilizing the fluorescence recovery after photobleaching technique (FRAP). The fluorescent signal was supplied by the Cy5 immobilized to the lipid coated particles. Particles were suspended in 1× PBS and incubated at 37 °C for the duration of the FRAP experiments. Using a Zeiss 780 FCS Confocal Microscope rectangular regions of interest were selected on a number of particles, these regions were bleached, following which the fluorescent recovery in the selected regions was tracked over time. The fluorescent intensity measured at each time point (I(t)) was then converted to a normalized fluorescent intensity (NFI(t)) using the following equation:

$$NFI(t) = \frac{I(t) - I_{post\ bleach}}{I_{pre\ bleach} * I_{post\ recovery}}$$

The NFI was then plotted against time and fit to a one phase exponential association curve using GraphPad Prism 7 (GraphPad Software, Inc.; La Jolla, CA). From the fit of the curves, time constants for half recovery were derived ($t_{0.5}$). In order to determine diffusion constants, we assumed a circular bleaching region in the spherical particles with a radius determined from ImageJ analysis the 2D images of post bleached particles (r_{bleach}). To account for the differences in surface area bleached in the spherical vs. ellipsoidal particles, we assumed the the area bleached in the ellipsoidal particles was an ellipse as opposed to a circle. The characteristic length was then taken to be the minor axis of the ellipse which was computed from measuring the major axis of the bleaching area by ImageJ in the 2D images and using an aspect ratio of 2.8 for the 2-fold stretched particles. [18] These values were then applied to the model set forth by Kang et al. [24] for derivation of lipid diffusion constants from FRAP:

$$D_{lipid} = \frac{r_{bleach}^2}{4 * t_{0.5}}$$

Diffusion constants for 10 particles for both shapes were computed with this model and compared.

2.7 Statistical analysis

All statistics were completed using statistical analysis software modules in GraphPad Prism 7 (GraphPad Software, Inc.; La Jolla, CA). For cellular uptake studies, differences in percent of cells positive for uptake and percent of cells positive for binding between the two shapes were evaluated using a Student's t-test. Significance was assumed if the p value of this test was less than 0.05. For avidin immobilization on particles and protein bound to the particles, a two-way ANOVA test was performed considering dose and shape as variables with interactions considered to be significant if the p value of the test was less than 0.05. Bonferroni's post-tests were performed to analyze differences between shapes at the various doses and the difference was considered significant with a p value less than 0.05. For cellular binding studies, the percent bound replicates were compared across the spherical and non-spherical shapes with and without anti-CD3 functionalization using a one way ANOVA with Tukey's post test to compare across groups. Significance was taken if the p value of this test was less than 0.05. The length of contact was compared between anti-CD3 functionalized and non-functionalized particles by a Student's t-test and significance was assumed if the p value of the test was less than 0.05. Lateral diffusion coefficients extracted from FRAP recovery curves were compared between particle shapes using a Student's t-test and significance was assumed if the p value of the test was less than 0.05.

3. Results

3.1 Lipid coated particle preparation and characterization

Spherical microparticles were generated (by homogenization of a PLGA/dichloromethane solution into a solution of 1% poly(vinyl alcohol)) and their size was measured by Image J analysis of scanning electron microscopy (SEM) micrographs (Fig 1a–b) and determined to be 3.2 μm +/− 1.2 μm in diameter (Fig 1c). We confirmed the maintenance of particle shape during the fabrication process by aspect ratio analysis of SEM micrographs of non-spherical particles coated with lipids (Fig 1b). The aspect ratio of the ellipsoidal particles was measured to be 3.3 +/− 0.6 (Fig 1d).

Confocal imaging of a representative batch of lipids on particles revealed that the 7-AMC fluorescence was confined to the interior of the particles for both spherical (Fig 2a) and ellipsoidal (Fig 2b) lipid coated particles, whereas the lipid-rhodamine signal was localized to the exterior of the particles in both cases. Profile analysis of each sample revealed that for both the spherical (Fig 2c) and the ellipsoidal particles (Fig 2d) that the maximum signal from the lipid-rhodamine conjugate was localized to the exterior of the particle utilizing the 7-AMC signal as a reference point.

3.2 Macrophage uptake of lipid coated particles

Particles, which were formulated encapsulating a fluorescent dye, were coated with lipids and conjugated to avidin via thiol/maleimide chemistry. The lipid coated particles were incubated with macrophages for four hours to permit phagocytosis to occur. Viability of the macrophages was unaltered during this incubation, as evidenced by a cell titer assay of both the spherical and ellipsoidal lipid coated particles at the end of 24 and 48 hrs. (Fig S1). At the conclusion of four hours, the macrophages were either fixed and stained for confocal imaging or removed from the plate by trituration for flow cytometry analysis.

Confocal imaging analysis yielded a qualitative comparison of spherical vs ellipsoidal lipid coated particle phagocytosis (Fig 3a vs. Fig 3b). In all cases examined by microscopy, spherical particles were phagocytosed at a higher rate and in greater number compared to the ellipsoidal particles. Quantitative flow cytometry analysis of the cells after four hours of particle treatment at 37 °C showed statistically significant inhibition of particle uptake with ellipsoidal shape compared to spherical shape at doses ranging from 7.8 μg particles per well (9.7% vs. 17.7% uptake) to 500 μg particles per well (43.1% vs. 61.2% uptake) in 96-well plates (Fig 3c). For cells incubated at 4 °C, there was a significant reduction in observed binding for the spherical particles compared to the ellipsoidal particles at the 500 μg and 250 μg dose.

3.3 Functionalization of lipid coated particles

To establish interchangeable functionalization of these particles, we employed a two-step coupling strategy. We first utilized a maleimide based conjugation to attach thiolated avidin to the surfaces of the particles followed by capture of biotinylated target biomolecules through the biotin-avidin interaction. In this manner, there is flexibility to attach any molecule to the surface that can be biotinylated, such as proteins or imaging agents. As proof of principle, we first functionalized the particles with biotinylated dye, biotinylated-Cy5. We independently confirmed that the avidin thiol was binding to the surface of the particles through incubating the particles with pre-fluorophore labeled avidin and assessing avidin content on the particles through fluorescence (Fig S2). As shown in the confocal micrographs of these spherical (Fig 4a) and ellipsoidal (Fig 4b) particles, the Cy5 signal was localized to the exterior of the particles using 7-AMC as a reference to denote the interior of the particles. We confirmed that the coupling of the biotinylated molecule is avidin specific by incubating particles with Cy-5 biotin but no avidin thiol. Confocal images demonstrate that the particles did not conjugate Cy5-biotin (Fig S3). Stability of the lipid coated particle to lyophilization (Fig S4) and extended exposure to 25 °C or 37 °C temperatures over a 7 day period (Fig S5) were evaluated and the particles experienced no measurable degradation in either case, demonstrating robustness of the fabrication of the anisotropic particles and their surface modification.

After verifying the reproducible capture of a biotinylated fluorophore by avidin conjugated to the surface of the lipid coated particles, we next evaluated the capture of a biotinylated antibody for murine CD28, an important costimulatory surface protein in the activation of lymphocytes. Through analysis of protein content in the supernatant of the wash steps, it was determined that the biotinylated antibody was captured on the surface of the particle and the

conjugation procedure was dose dependent (Fig 4c). In addition, the efficiency of conjugation was evaluated to be 50–70%, across the doses of protein in synthesis (Fig 4d). These experiments demonstrate the flexibility and efficiency of incorporating target biomolecules onto the surfaces of these anisotropic particles by simple mixing at room temperature.

3.4 Cellular binding of lipid coated particles

To determine the capability of ellipsoidal microparticles to bind to cells in a targeted manner, we incubated the anti-CD3 conjugated microparticles loaded with TAMRA with Jurkat T-Cells labeled with CFSE. Confocal imaging of the particle samples revealed the presence of conjugates between the particles and cells only in the presence of anti-CD3 (Fig 5a–d). Moreover the ellipsoidal particles visually appeared to interact with cells along the long axis of the ellipsoidal particles (Fig 5d). Multiple confocal images were taken of the samples and using ImageJ, the number of conjugates per number of cells was determined for all four samples. This percentage was found to be significantly higher in the ellipsoidal lipid coated particle with anti-CD3 compared to the spherical with anti-CD3 and both shapes not coated with antibody (Fig 5e). Futhermore, using ImageJ to measure the length of contact between the particle and the cell, it was found that the ellipsoidal lipid coated particles with anti-CD3 had a significantly higher length of contact with the cells than the spherical particles with anti-CD3 (Fig 5f).

3.5 Lateral membrane fluidity of particle supported lipids

To assess particle surface fluidity, we utilized fluorescence recovery after photobleaching (FRAP). Briefly, a particle was first located under confocal microscopy and a small circular region of the lipid layer approximately 1 μm in diameter was identified and bleached as described in the Methods section. The resulting bleached region was monitored over time and the recovery of the fluorescence signal was measured as labeled lipids diffused into the photobleached zone. Both spherical (Fig 6a) and ellipsoidal (Fig 6b) particles showed close to complete recovery of fluorescence within 150 s, using this data. Diffusion constants were determined by a normalization and fit of the signal recovery data (Fig 6c). Both spherical and ellipsoidal particles had statistically similar diffusion constants that were also on the same order of magnitude (10^{-10} cm^2s^{-1}) as those observed for proteins on natural, biological membranes [25]. This value of surface diffusivity is important for applications where mimicry of biological membranes is desired, such as to emulate the diffusion and clustering of receptors found on natural cellular surfaces.

4. Discussion

Validation of our ability to generate ellipsoidal and spherical lipid coated particles utilizing poly(lactic-co-glycolic) acid (PLGA) for polymeric structural support is provided in Figure 1. As determined by aspect ratio analysis, our average aspect ratio was 3.3 for the stretched particles. This is near the predicted value of 2.8 as computed for a spherical particle that is stretched two-fold in a thin film [18]. To confirm the fabrication of lipid coated particles, and the ability to encapsulate cargo within the particles as well as coupled to the lipid surface, PLGA microparticles encapsulating 7-amino-4-methyl coumarin (7-AMC) were

first made to visualize the core of the lipid polymer hybrid particle. After thin film stretching, the particles were coated with fluorescent liposomes containing rhodamine and imaged using confocal microscopy. We could visualize an enrichment of rhodamine signal around the outside of the particle. Furthermore, the encapsulated dye was also visible and determined to be localized to the center. This demonstrates that our spherical or ellipsoidal lipid coated particle platform has the ability to be used in the delivery of small hydrophobic drugs or contrast agents as has been demonstrated previously in other biodegradable particle platforms [26, 27].

The biomimetic properties of lipid coated non-spheroidal particles may have precluded a hypothesized advantage of the ellipsoidal lipid coated particle constructs, namely their capability to reduce non-specific uptake compared to spherical particles of the same volume and mass. Therefore, upon validation of non-spheroidal lipid coated particle synthesis, the next goal was to investigate non-specific uptake of the ellipsoidal lipid coated particles. As demonstrated with confocal imaging, both spherical and ellipsoidal particles were capable of being internalized. However, there was a noted difference between the spherical and ellipsoidal samples. Across multiple doses of particles administered to the cells, there was a statistically significant decrease in internalization rate of ellipsoidal lipid coated particles compared to spherical lipid coated particles. Furthermore, the binding of particles was significantly reduced in the spherical compared to the ellipsoidal lipid coated particles suggesting this observed uptake difference was from differences in quantities of internalized particles, not non-specific adherence of the particles to the cell membranes. This trend, which has previously been described in the literature for non-lipid coated polymeric particles with varied shape [12] confirms that our newly developed ellipsoidal lipid coated particles maintain the advantageous biological properties of non-spherical anisotropic particles [28]. Viability of the macrophages was unaltered during this incubation, as evidenced by a cell titer assay of both the spherical and ellipsoidal lipid coated particles, indicating that these lipid coated particles do not exhibit non-specific cytotoxic effects.

Upon confirmation that the lipid coating did not negate the key advantage of reduced non-specific uptake, we next demonstrated that our technique was compatible with a flexible conjugation strategy of attaching biomolecules such as protein to the surface of the anisotropic lipid coated particles under gentle conditions. For many applications, such as cell type-specific targeting, this approach involves the conjugation of antibodies that recognize tumor-associated antigens (TAAs) to the supported lipids. In other cases, fluorescent moieties are conjugated to the particle to assist in the visualization and imaging of the particle or to study the fluidic properties of the lipid coating. To achieve a robust and versatile platform for the presentation of any target protein or small molecule for applications such as drug delivery, gene delivery, and immunoengineering, we utilized maleimide functionalized lipids during the liposome synthesis and then conjugated thiolated avidin (that had been pre-bound to biotinylated fluorescein) to the surface of the lipid coated particles. Once lipids are functionalized with avidin, they become a versatile platform for conjugation of any biotinylated moiety, which we demonstrated using biotinylated Cy5 fluorophore and a biotinylated immunologically relevant antibody (anti-CD28). We did not note a plateau in the amount of protein immobilized on the surface, however the amount that

could be conjugated is significantly high enough to elicit a physiological response from T-Cells. [18]

One of the key advantages of ellipsoidal micro and nanoparticles compared to their spherical equivalents is the ability to bind more efficiently in a targeted fashion. This has been attributed to the higher radius of curvature of ellipsoidal particles compared to spherical particles and subsequently more surface area available for interaction with the cell. [29] This has been shown both *in vitro* and *in vivo* to enhance the accumulation of ellipsoidal particles at targeted binding sites compared to spherical particles. [30] We have demonstrated in this study that this highly advantageous shape mediated targeting property is preserved with the anisotropic lipid coated particle system. We utilized anti-CD3, an immunostimualtory ligand, to target the binding of the spherical and ellipsoidal lipid coated particles to T-Cells. Both the amount of cells bound to particles and the length of contact between particles and cells were enhanced with the ellipsoidal lipid coated particles compared to the spherical lipid coated particles. This trend has been reported in the literature with similar sized particles and was found to be correlated with a significant increase in antigen specific immune stimulation. [18]

An important biomimetic feature of the supported lipids is their membrane fluidity. One instance where this has been determined to be important is in the presentation of immunostimulatory ligands by artificial antigen presenting cells. Natural antigen presenting cells undergo dynamic rearrangement of their surface receptors upon engagement with a cognate T-Cell, and the lateral fluidity of these T-Cells has been deemed important for T-Cell activation [5]. To that end we were interested in evaluating the fluidity of the new spherical and ellipsoidal lipid coated particles utilizing an established fluorescence recovery after photobleaching technique (FRAP) [2]. Both spherical and ellipsoidal particles had statistically similar diffusion constants that were also on the same order of magnitude (10^{-10} cm^2s^{-1}) as those observed for proteins on natural, biological membranes [25]. For a supported lipid bilayer on glass, this diffusion constant is significantly lower than the average of 10^{-8} cm^2s^{-1}. However, it is worth noting that diffusion constants for supported lipid bilayers on non-glass substrates are typically lower than this number. For example, Sterling et. al. demonstrated that lipids deposited on actin coated glass slides had diffusion coefficients 50% lower than lipids on uncoated glass. [31] Furthermore, Scomparin et. al. compared lipids deposited on glass and mica and noted an order of magnitude drop in the diffusion constant for lipids coated on mica compared to glass. [32] Some of these reported diffusion constants were also in the range of our finding of 10^{-10} cm^2s^{-1}. This is significant as through these studies, these new anisotropic, synthetic biodegradable particles, are now demonstrated to mimic natural biological cells in four important ways: 1) Biological micron length-scale size, 2) Anisotropic shape and (via the automated stretching device) tunable radius of curvature, 3) Fluid lipid surface (with biomimetic diffusivity), and 4) facile incorporation/presentation of protein from the lipid surface. These artificial biomimetic particles as a biomaterial may be useful for varied biomedical applications.

5. Conclusion

In conclusion, we have successfully developed a procedure to synthesize biomimetic anisotropic lipid coated particles. By combining fabrication procedures for biodegradable particle synthesis, thin film stretching, lipid coating, and flexible biomolecular conjugation, we have enabled the capability for modular surface presentation of biologically relevant proteins on a fluidic synthetic lipid membrane of defined anisotropic geometry. Critically, we have verified that this platform maintains the advantageous aspects of the non-spherical particle, specifically the capability to resist macrophage phagocytosis. In addition, this protein presentation reproduces the dynamic membrane properties of living cells and can be supported by particles of different shapes and tunable radius of curvature. This biotechnology can allow for more accurate mimicry of natural cells through the presentation of laterally mobile proteins on the surface of anisotropic biodegradable particles, while enabling independent control of the geometry of the particle, and enabling encapsulation of biological cargos. Therefore, this biomaterial platform may be of great benefit for varied applications including imaging and therapy.

Supplementary Material

Refer to Web version on PubMed Central for supplementary material.

Acknowledgments

The authors thank the JHU-Coulter Translational Partnership, the TEDCO Maryland Innovation Initiative, and the NIH (R01-EB016721, R01- CA195503, and P30-EY001765). RAM thanks the Achievement Rewards for College Scientists (ARCS) and the National Cancer Institute of the NIH (F31CA214147) for fellowship support.

References

1. Wang H, Zhao P, Su W, Wang S, Liao Z, Niu R, Chang J. PLGA/polymeric liposome for targeted drug and gene co-delivery. Biomaterials. 2010; 31:8741–8748. [PubMed: 20727587]
2. Bershteyn A, Chaparro J, Yau R, Kim M, Reinherz E, Ferreira-Moita L, Irvine DJ. Polymer-supported lipid shells, onions, and flowers. Soft Matter. 2008; 4:1787–1791. [PubMed: 19756178]
3. Hadinoto K, Sundaresan A, Cheow WS. Lipid–polymer hybrid nanoparticles as a new generation therapeutic delivery platform: a review. Eur J. Pharm. Biopharm. 2013; 85:427–443. [PubMed: 23872180]
4. Cheow WS, Hadinoto K. Factors affecting drug encapsulation and stability of lipid–polymer hybrid nanoparticles. Colloid. Surface. B. 2011; 85:214–220.
5. Mieszawska AJ, Gianella A, Cormode DP, Zhao Y, Meijerink A, Langer R, Farokhzad OC, Fayad ZA, Mulder WJ. Engineering of lipid-coated PLGA nanoparticles with a tunable payload of diagnostically active nanocrystals for medical imaging. Chem. Comm. 2012; 48:5835–5837. [PubMed: 22555311]
6. Xu J, Luft JC, Yi X, Tian S, Owens G, Wang J, Johnson A, Berglund P, Smith J, Napier ME, DeSimone JM. RNA replicon delivery via lipid-complexed PRINT protein particles. Mol. Pharm. 2013; 10:3366–3374. [PubMed: 23924216]
7. Hasan W, Chu K, Gullapalli A, Dunn SS, Enlow EM, Luft JC, Tian S, Napier ME, Pohlhaus PD, Rolland JP, DeSimone JM. Delivery of multiple siRNAs using lipid-coated PLGA nanoparticles for treatment of prostate cancer. Nano Lett. 2012; 12:287–292. [PubMed: 22165988]
8. Hu C-MJ, Zhang L, Aryal S, Cheung C, Fang RH, Zhang L. Erythrocyte membrane-camouflaged polymeric nanoparticles as a biomimetic delivery platform. Proc. Natl. Acad. Sci. U. S. A. 2011; 108:10980–10985. [PubMed: 21690347]

9. Hu C-MJ, Fang RH, Wang K-C, Luk BT, Thamphiwatana S, Dehaini D, Nguyen P, Angsantikul P, Wen CH, Kroll AV. Nanoparticle biointerfacing by platelet membrane cloaking. Nature. 2015; 526:118–121. [PubMed: 26374997]
10. Fang RH, Hu C-MJ, Luk BT, Gao W, Copp JA, Tai Y, O'Connor DE, Zhang L. Cancer cell membrane-coated nanoparticles for anticancer vaccination and drug delivery. Nano Lett. 2014; 14:2181–2188. [PubMed: 24673373]
11. Hu C-MJ, Fang RH, Copp J, Luk BT, Zhang L. A biomimetic nanosponge that absorbs pore-forming toxins. Nat. Nanotechnol. 2013; 8:336–340. [PubMed: 23584215]
12. Sharma G, Valenta DT, Altman Y, Harvey S, Xie H, Mitragotri S, Smith JW. Polymer particle shape independently influences binding and internalization by macrophages. J. Control. Release. 2010; 147:408–412. [PubMed: 20691741]
13. Canelas DA, Herlihy KP, DeSimone JM. Top-down particle fabrication: control of size and shape for diagnostic imaging and drug delivery. WIREs: Nanomed. Nanobiotechnol. 2009; 1:391–404.
14. Karagoz B, Esser L, Duong HT, Basuki JS, Boyer C, Davis TP. Polymerization-Induced Self-Assembly (PISA) – control over the morphology of nanoparticles for drug delivery applications. Polym. Chem. 2014; 5:350.
15. Chu KS, Finniss MC, Schorzman AN, Kuijer JL, Luft JC, Bowerman CJ, Napier ME, Haroon ZA, Zamboni WC, DeSimone JM. Particle replication in nonwetting templates nanoparticles with tumor selective alkyl silyl ether docetaxel prodrug reduces toxicity. Nano Lett. 2014; 14:1472–1476. [PubMed: 24552251]
16. Jiang X, Leong D, Ren Y, Li Z, Torbenson MS, Mao HQ. String-like micellar nanoparticles formed by complexation of PEG-b-PPA and plasmid DNA and their transfection efficiency. Pharm. Res. 2011; 28:1317–1327. [PubMed: 21499836]
17. Jiang X, Qu W, Pan D, Ren Y, Williford JM, Cui H, Luijten E, Mao HQ. Plasmid-templated shape control of condensed DNA-block copolymer nanoparticles. Adv. Mater. 2013; 25:227–232. [PubMed: 23055399]
18. Sunshine JC, Perica K, Schneck JP, Green JJ. Particle shape dependence of CD8+ T cell activation by artificial antigen presenting cells. Biomaterials. 2014; 35:269–277. [PubMed: 24099710]
19. Meyer RA, Sunshine JC, Perica K, Kosmides AK, Aje K, Schneck JP, Green JJ. Biodegradable Nanoellipsoidal Artificial Antigen Presenting Cells for Antigen Specific T-Cell Activation. Small. 2015; 11:1519–1525. [PubMed: 25641795]
20. Champion JA, Katare YK, Mitragotri S. Particle shape: a new design parameter for micro- and nanoscale drug delivery carriers. J. Control. Release. 2007; 121:3–9. [PubMed: 17544538]
21. Ho C, Keller A, Odell J, Ottewill R. Preparation of monodisperse ellipsoidal polystyrene particles. Colloid Polym. Sci. 1993; 271:469–479.
22. Meyer RA, Meyer RS, Green JJ. An automated multidimensional thin film stretching device for the generation of anisotropic polymeric micro-and nanoparticles. J. Biomed. Mater. Res. Part A. 2015
23. Ashley CE, Carnes EC, Phillips GK, Padilla D, Durfee PN, Brown PA, Hanna TN, Liu J, Phillips B, Carter MB. The targeted delivery of multicomponent cargos to cancer cells by nanoporous particle-supported lipid bilayers. Nat. Mater. 2011; 10:389–397. [PubMed: 21499315]
24. Kang M, Day CA, Kenworthy AK, DiBenedetto E. Simplified equation to extract diffusion coefficients from confocal FRAP data. Traffic. 2012; 13:1589–1600. [PubMed: 22984916]
25. Lenaz G. Lipid fluidity and membrane protein dynamics. Bioscience Rep. 1987; 7:823–837.
26. Sun T, Zhang YS, Pang B, Hyun DC, Yang M, Xia Y. Engineered nanoparticles for drug delivery in cancer therapy. Angew. Chem. Int. Edit. 2014; 53:12320–12364.
27. Mariano RNsAlberti D, Cutrin JC, Geninatti Crich S, Aime S. Design of PLGA based nanoparticles for imaging guided applications. Mol. Pharm. 2014; 11:4100–4106. [PubMed: 25225751]
28. Meyer RA, Green JJ. Shaping the future of nanomedicine: anisotropy in polymeric nanoparticle design. WIREs: Nanomed. Nanobiotechnol. 2015
29. Toy R, Peiris PM, Ghaghada KB, Karathanasis E. Shaping cancer nanomedicine: The effect of particle shape on the *in vivo* journey of nanoparticles. Nanomed. 2014; 9:121–134.

30. Kolhar P, Anselmo AC, Gupta V, Pant K, Prabhakarpandian B, Ruoslahti E, Mitragotri S. Using shape effects to target antibody-coated nanoparticles to lung and brain endothelium. Proc. Natl. Acad. Sci. U. S. A. 2013; 110:10753–10758. [PubMed: 23754411]

31. Sterling SM, Dawes R, Allgeyer ES, Ashworth SL, Neivandt DJ. Comparison Actin- and Glass-Supported Phospholipid Bilayer Diffusion Coefficients. Biophys. J. 2015; 108:1946–1953. [PubMed: 25902434]

32. Scomparin C, Lecuyes S, Ferreira M, Charitat T, Tinland B. Diffusion in supported lipid bilayers: Influence of substrate and preparation technique on the internal dynamis. Eur. Phys. J. 2009; 28:211–220.

Statement of Significance

The research reported here documents the ability of non-spherical polymeric particles to be coated with lipids to form anisotropic biomimetic particles. In addition, we demonstrate that these lipid-coated biodegradable polymeric particles can be conjugated to a wide variety of biological molecules in a “click-like” fashion. This is of interest due to the multiple types of cellular mimicry enabled by this biomaterial based technology. These features include mimicry of the highly anisotropic shape exhibited by cells, surface presentation of membrane bound protein mimetics, and lateral diffusivity of membrane bound substrates comparable to that of a plasma membrane. This platform is demonstrated to facilitate targeted cell binding while being resistant to non-specific cellular uptake. Such a platform could allow for investigations into how physical parameters of a particle and its surface affect the interface between biomaterials and cells, as well as provide biomimetic technology platforms for drug delivery and cellular engineering.

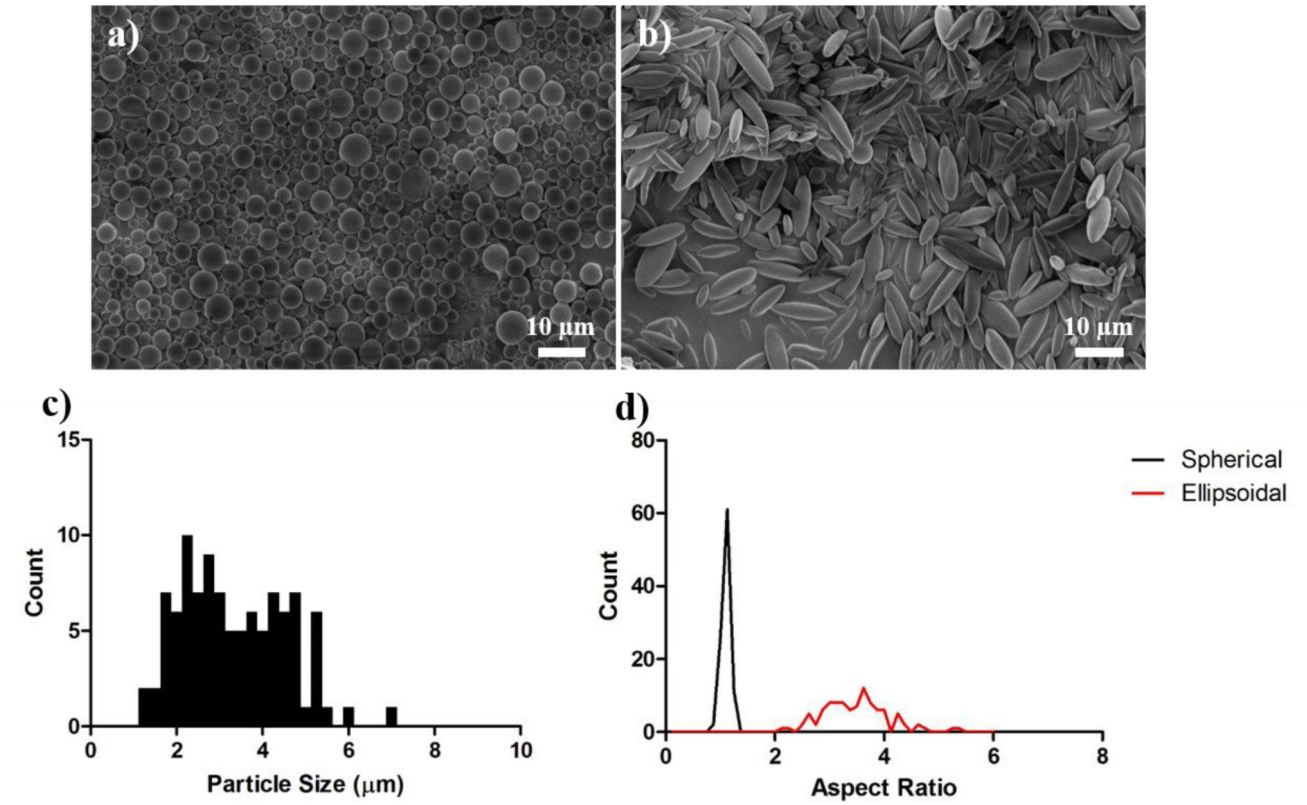

Figure 1.

Spherical and non-spherical particles utilized for the synthesis of lipid coated particles. SEM images of (a) spherical and (b) ellipsoidal microparticles utilized as templates for the support of the lipids. (c) Size of spherical particles and (d) measured aspect ratio of spherical and ellipsoidal particles.

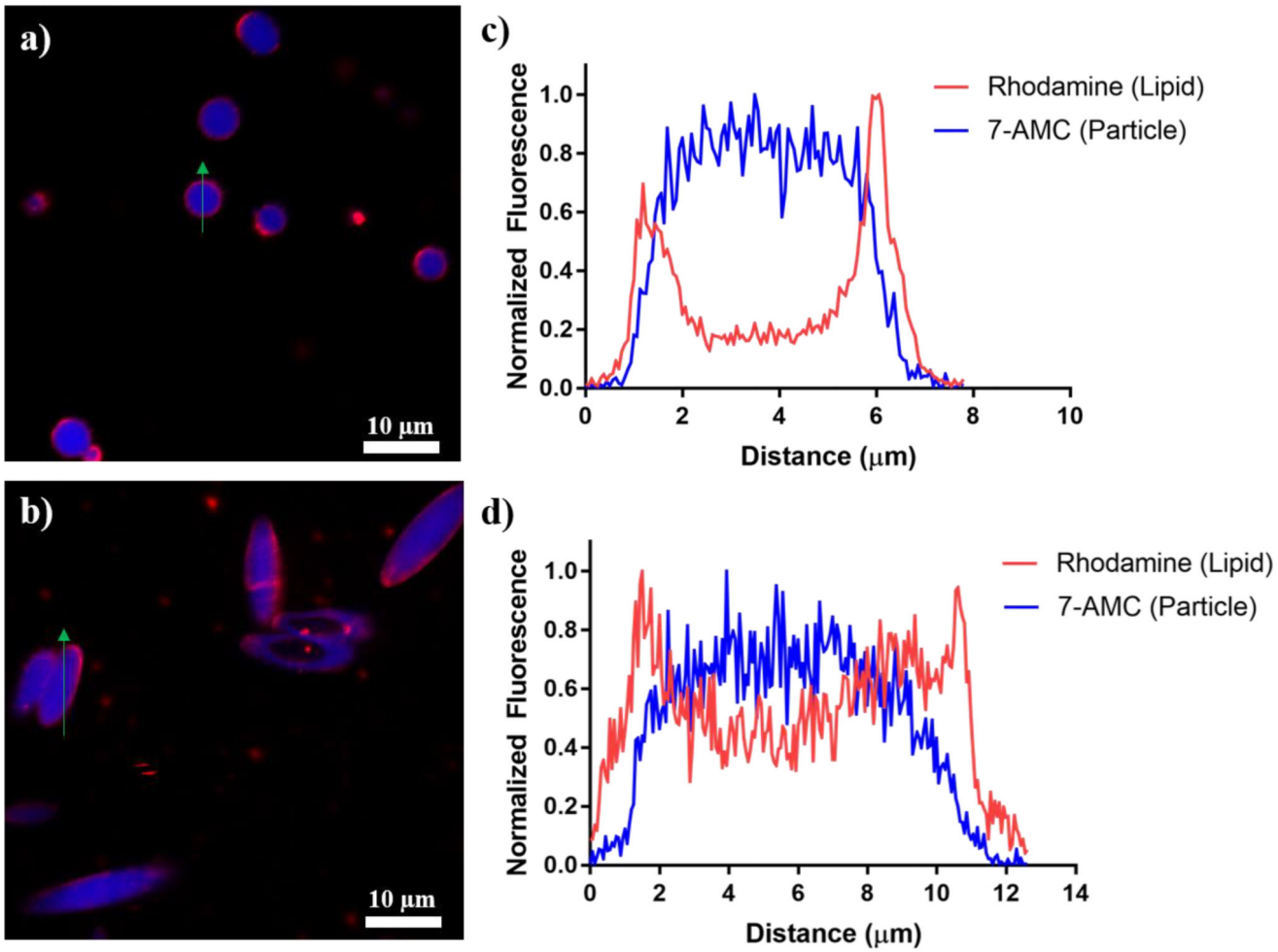

Figure 2.

Ellipsoidal and spherical lipid coated particles can be synthesized utilizing a preformed particle template. Confocal micrographs of (a) spherical and (b) ellipsoidal particles encapsulating 7-AMC (blue) coated with a fluorescent lipids (red). Representative profile of the two fluorescence channels across the (c) center of the sphere and the (d) long axis of the ellipsoid. Green arrows on (a) and (b) denote where the profile was taken.

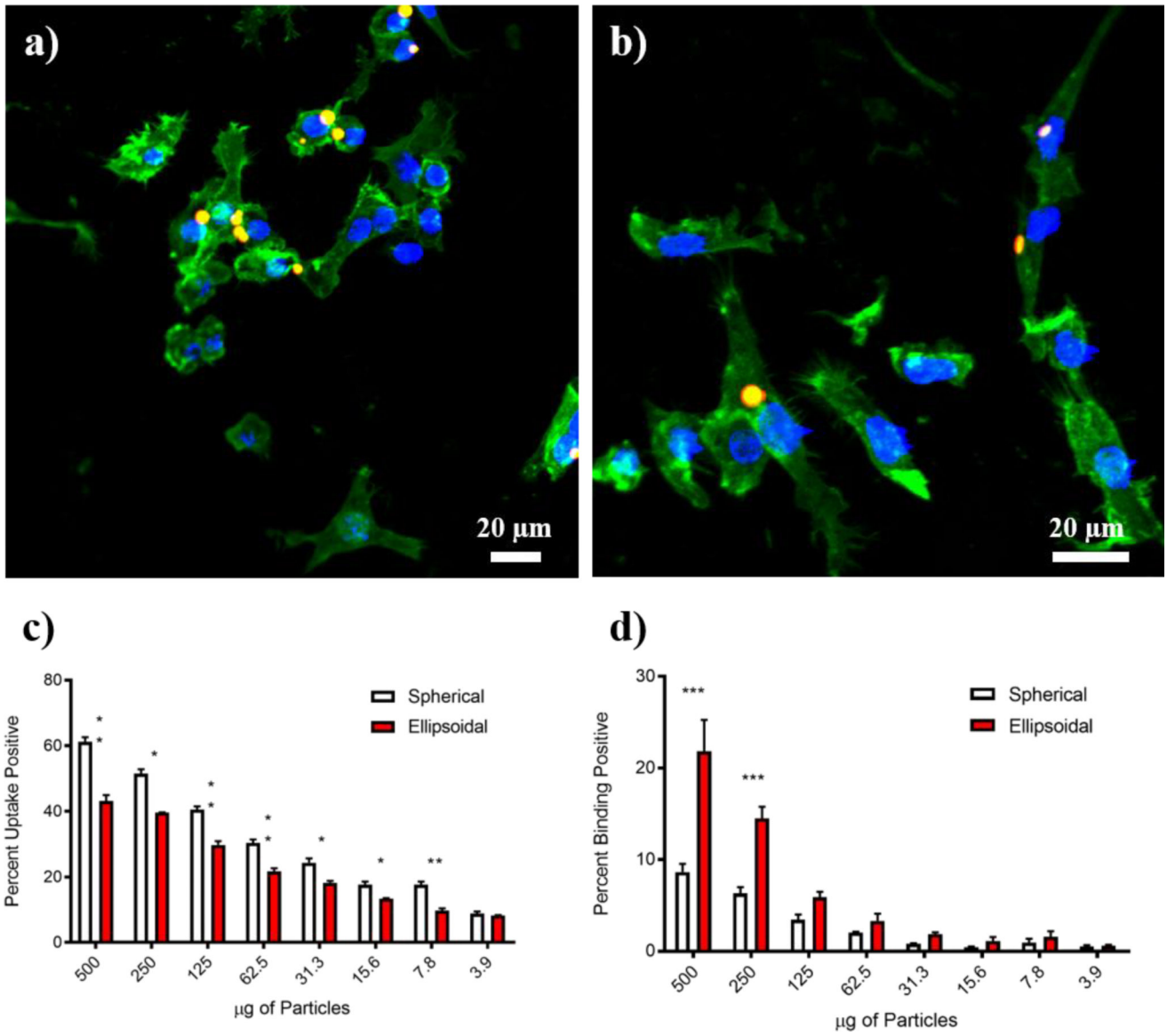

Figure 3.

Macrophage uptake is shape dependent for spherical and ellipsoidal lipid coated particles. Confocal micrographs of non-specific uptake of (a) spherical and (b) ellipsoidal lipid coated particles (red) by macrophages (green = actin, blue = DAPI) demonstrates that ellipsoids resist non-specific cell uptake. Flow cytometry of macrophages treated with lipid coated particles at (c) 37 °C and (d) 4 °C of spherical and ellipsoidal shape reinforce the conclusion that ellipsoidal lipid coated particles resist cellular uptake. (* = $p<0.05$, ** = $p<0.01$, *** = $p<0.001$, **** = $p<0.0001$)

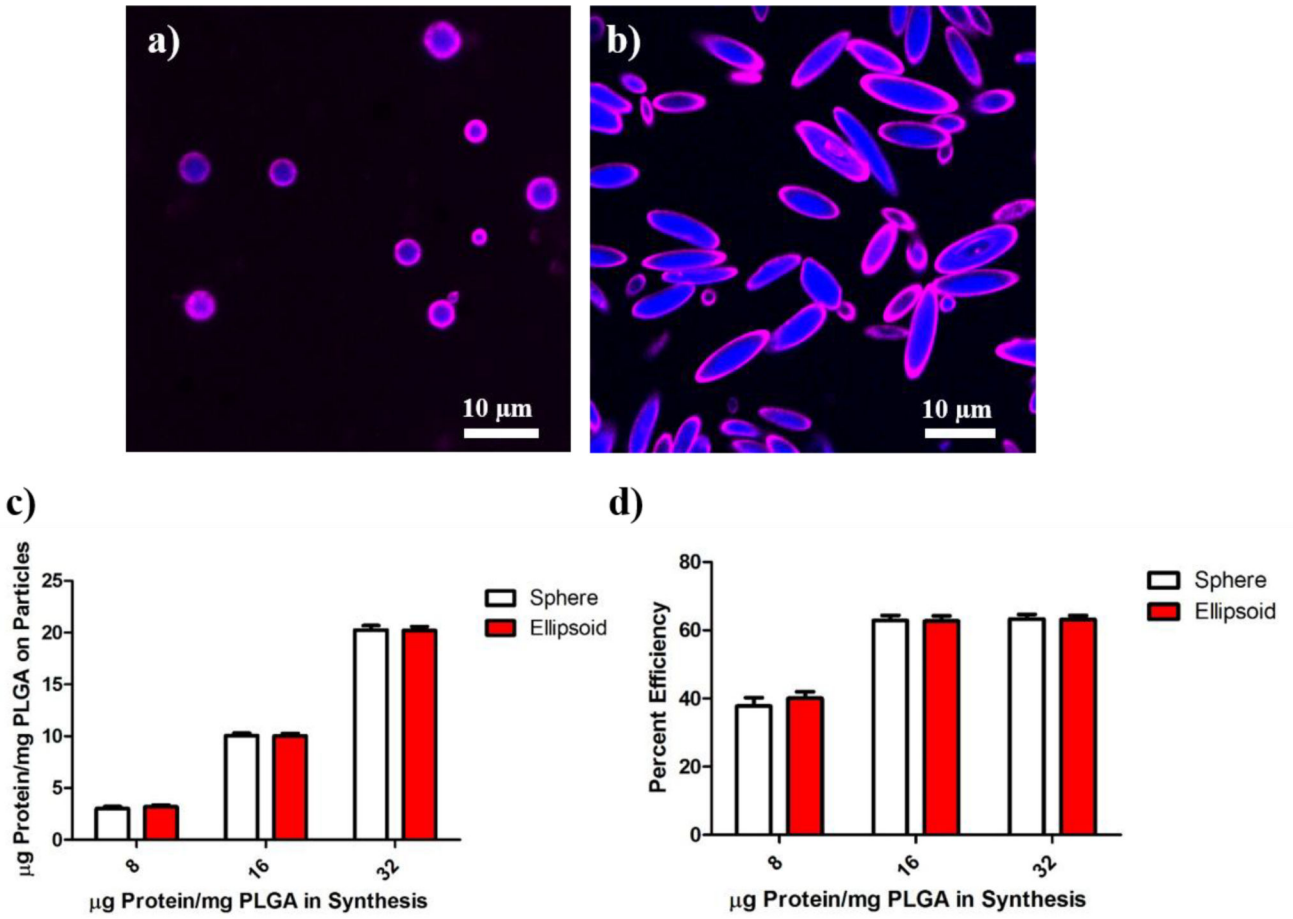

Figure 4.

Interchangeable protein surface conjugation to spherical and non-spherical lipid coated particles. (a) Spherical and (b) ellipsoidal lipid coated particles encapsulating 7-AMC (blue) conjugated to avidin-biotin-fluorophore (magenta) conjugated on the surface. (c) Total protein captured by particles exhibits dependency on the amount of protein dosed in synthesis. (d) Efficiency of conjugation between spherical and non-spherical lipid coated particles at various doses is similar. Error bars represent SEM of 3 replicates.

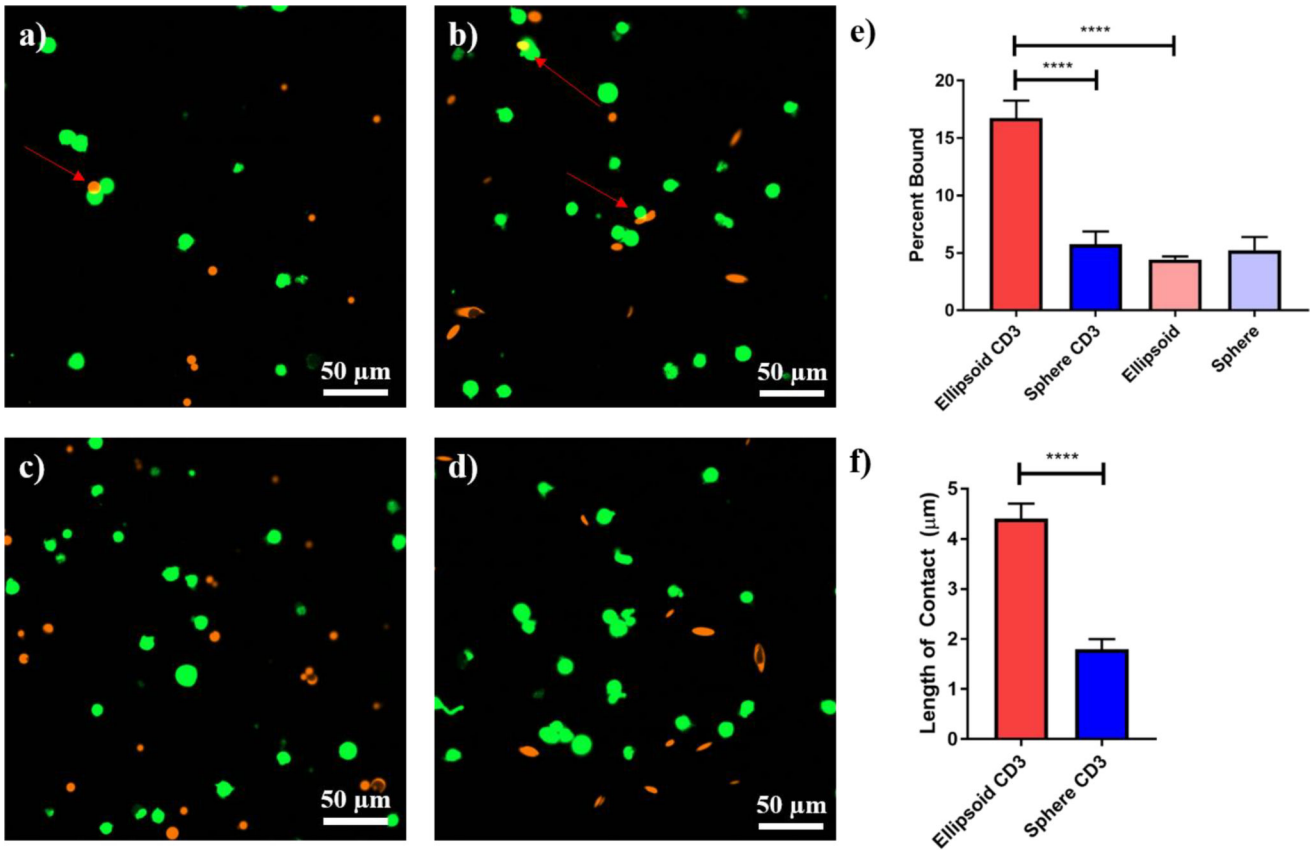

Figure 5.

Targeted cell binding is shape dependant for lipid coated particles. Jurkat T-Cells were incubated with spherical or ellipsoidal anti-CD3 conjugated lipid coated particles or unconjugated lipid coated particles. Confocal images of (a) anti-CD3 spherical, (b) anti-CD3 ellipsoidal, (c) blank spherical, and (d) blank ellipsoidal particles demonstrate enhanced binding of ellipsoidal anti-CD3 lipid coated microparticles (red arrows denote instances of binding). Images were quantified by ImageJ for (e) frequency of cells bound to particles and (f) length of contact between particles and cells. Ellipsoidal anti-CD3 outperformed other conditions in both of these analyses. Error barts represent SEM of 10 image analyses. (**** = $p<0.0001$)

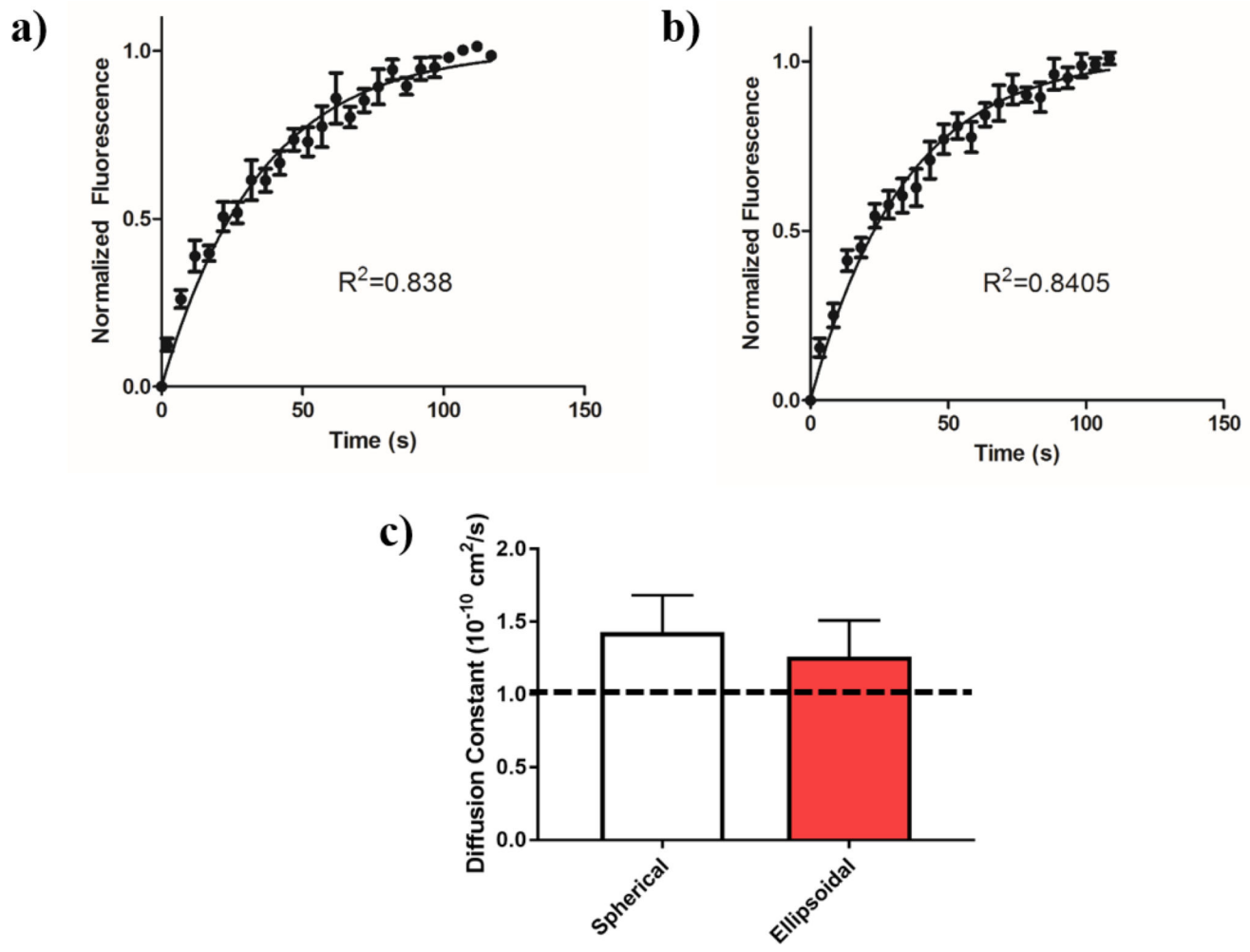

Figure 6.

Lipid coated particles bearing conjugated molecules demonstrate fluidity. (a) Spherical lipid coated particles and (b) ellipsoidal lipid coated particles were subjected to region specific bleaching under confocal microscopy and subsequently imaged to measure recovery of fluorescence. From an exponential fit of the recovery of the lipid signal, (c) lateral diffusion constants were derived for the spherical and ellipsoidal lipid coated particles and were determined to be equivalent. The dotted line represents a reported lateral diffusion coefficient value for membrane bound proteins in a natural cell.

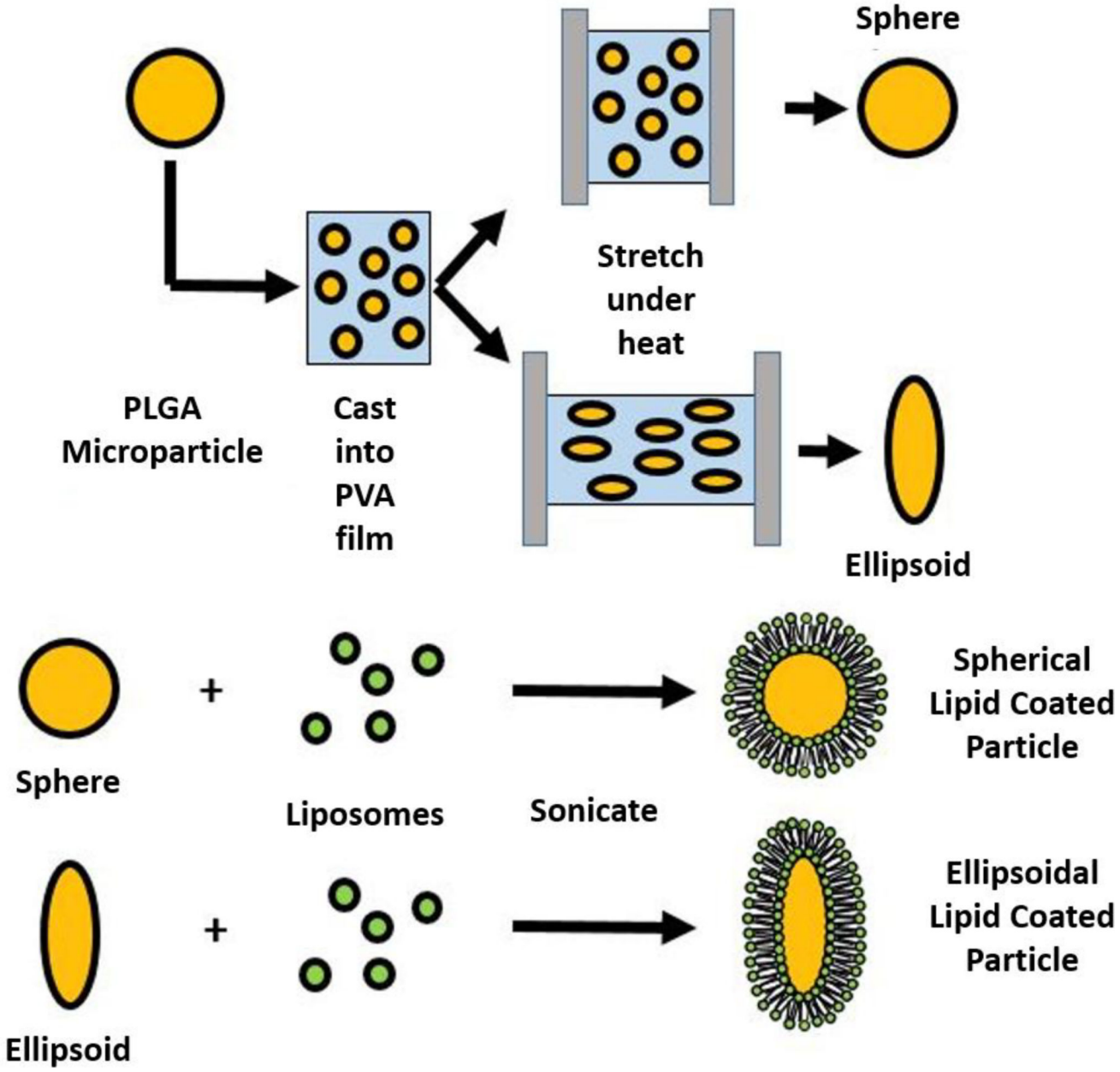

Scheme 1.

Schematic representation of ellipsoidal and spherical lipid coated particle synthesis. (a) Ellipsoidal microparticles were prepared utilizing a thin film stretching method starting from spherical PLGA microparticles prepared by single emulsion. (b) Liposomes that ~200 nm in size were prepared by extrusion and then sonicated in the presence of microparticles to yield lipid coated particles with shape specified by the initial particle template.

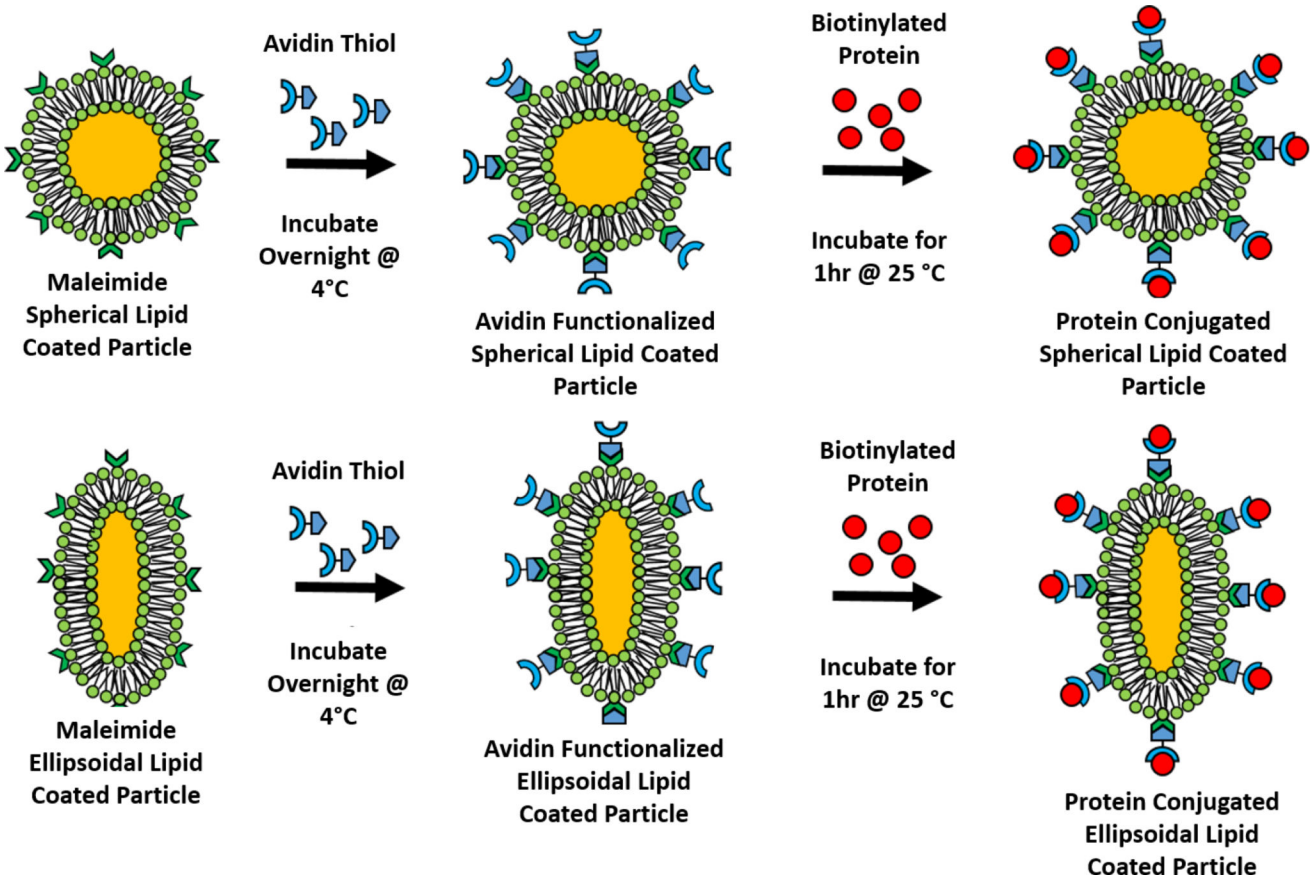

Scheme 2.

Functionalization strategy for lipid coated particles. (a) Lipid coated particles were synthesized on both spherical and ellipsoidal microparticles containing maleimide activated lipids. These maleimide lipids were reacted overnight at 4 °C with thiolated avidin to produce (b) lipid coated particles with avidin on the surface. These avidin functionalized lipids were then reacted with biotinylated molecules (either a fluorophore or protein) to produce (c) the final functional product.